NJC

Accepted Manuscript

This article can be cited before page numbers have been issued, to do this please use: M. Peric, M. Radovi, M. D. Mirkovi, A. S. Nikolic, P. Iskrenovi, D. Jankovic and S. Vranješ Djuri, *New J. Chem.*, 2019, DOI: 10.1039/C8NJ06478D.

This is an Accepted Manuscript, which has been through the Royal Society of Chemistry peer review process and has been accepted for publication.

Accepted Manuscripts are published online shortly after acceptance, before technical editing, formatting and proof reading. Using this free service, authors can make their results available to the community, in citable form, before we publish the edited article. We will replace this Accepted Manuscript with the edited and formatted Advance Article as soon as it is available.

You can find more information about Accepted Manuscripts in the author guidelines.

Please note that technical editing may introduce minor changes to the text and/or graphics, which may alter content. The journal's standard Terms & Conditions and the ethical guidelines, outlined in our author and reviewer resource centre, still apply. In no event shall the Royal Society of Chemistry be held responsible for any errors or omissions in this Accepted Manuscript or any consequences arising from the use of any information it contains.

ROYAL SOCIETY OF CHEMISTRY

rsc.li/njc

Journal Name

ROYAL SOCIETY OF CHEMISTRY
View Article Online
DOI: 10.1039/C8NJ06478D

ARTICLE

The analysis of the 2,3-dicarboxypropane-1,1-diphosphonic acid coated magnetite nanoparticles in the external magnetic field and their radiolabeling for possible theranostic application

Received 00th January 20xx,
Accepted 00th January 20xx

DOI: 10.1039/x0xx00000x

www.rsc.org/

Marko Perić*[a], Magdalena Radović[a], Marija Mirković[a], Aleksandar S. Nikolić[b], Predrag Iskrenović[c], Drina Janković[a] and Sanja Vranješ-Đurić[a]

The advances in nanotechnology are directed toward development of new theranostic agents based on magnetic nanoparticles that can be used for both cancer detecting and treating. In this study, 2,3-dicarboxypropane-1,1-diphosphonic acid coated magnetite nanoparticles (Fe_3O_4-DPD MNPs) were evaluated for the theranostic application by using different methods. The magnetic hyperthermia efficiency of Fe_3O_4-DPD MNPs was investigated in saline solution with ionic strenghts between 0.05-1.0 mol/dm^3. For better understanding of hyperthermia, the behavior of Fe_3O_4-DPD MNPs in the non-alternating magnetic field was followed by measuring the transparency of the sample. Furthermore, the radiotracer method using radionuclides ^{99m}Tc and ^{90}Y was applied as a reliable and powerful method for evaluating the *in vivo* behavior of a nanoprobe. High radiolabeling yield (>93 %), *in vitro* and *in vivo* stability of radiolabeled nanoparticles and high heating effect, paving the way for the possible theranostic application of Fe_3O_4-DPD MNPs.

1 Introduction

The rapid development of nanotechnology enabled biomedical application of large number of newly emerged nanomaterials. Magnetic nanoparticles (MNPs) offer several opportunities in the application including the magnetic resonance imaging (MRI), hyperthermia treatment of malignant tissues, site-specific drug/radionuclide delivery and therefore they represent powerful theranostic agent.[1]

During magnetic hyperthermia treatment, MNPs are exposed to an alternating magnetic field (MF), generating the heat due to the magnetic hysteresis loss mechanism and *Brownian* and *Neel* relaxation phenomena.[2,3] Temperature between 42-46 °C induce changes in the protein metabolism that may finally result in cellular degradation and apoptosis of the cancer cells while causing minimal damage to the surrounding healthy cells.[4] Hyperthermia treatment is usually used in combination with other cancer therapy options such as radiotherapy or chemotherapy because the simultaneous delivery of heat and radionuclides/drugs is much more effective in achieving therapeutic effects.[5] Furthermore, multifunctional radiolabeled MNPs nanoparticles with the capability of detecting and destroying of cancer cells with the potential for the visualization of therapy have been considered as the best choice for the application in cancer therapy.[6] Radiolabeling of MNPs with gamma or positron emitters allows combined hyperthermia treatment and MRI/PET or MRI/SPECT imaging.[7,8] In contrast, labeling with beta emitters provides an opportunity for MRI diagnostic and dual hyperthermia-radionuclide therapy.

The biomedical applications of MNPs depend on their colloidal and chemical stability and aggregation levels in physiological conditions. The ionic and protein composition of biological media has strong influence on the physicochemical and biological behavior of MNPs.[9,10] To improve biocompatibility and colloidal stability of MNPs in biological systems appropriate surface coatings is necessary.[11] To the best of our knowledge, there is a small number of studies using bisphosphonates (BPs) as coatings in spite of their great affinity towards metal ions and biocompatibility.[12,13] Bisphosphonates are well-known drugs in osteoporosis and oncology due to the high binding affinity to the surface of the metabolically active bone. The 2,3-dicarboxypropane-1,1-diphosphonic acid (DPD) is water soluble and biocompatible bisphosphonate which provide suitable dispersion stability and reduces the cytotoxicity of the naked Fe_3O_4 MNPs.[6,7] In addition, DPD as a tetradentate ligand, serves as an effective chelator. Complex DPD with ^{99m}Tc has been widely accepted for bone scintigraphy because of its high sensitivity and easy evaluation of the whole skeletal system.[14] Also, DPD is capable to form stable complexes with ^{90}Y.[15] Conjugation of DPD to the surface of iron oxide MNPs and their labeling with ^{68}Ga, make them suitable for PET/MRI imaging.[7]

[a] Vinča Institute of Nuclear Sciences, University of Belgrade, P. O. BOX 522, Belgrade, Serbia
[b] Faculty of Chemistry, University of Belgrade, Studentski Trg 12–16, 11001 Belgrade, Serbia
[c] Faculty of Physics, University of Belgrade, Studentski Trg 12, 11001 Belgrade, Serbia
[d] † Corresponding author E-mail: markop@chem.bg.ac.rs.

View Article Online DOI: 10.1039/C9NJ00647D

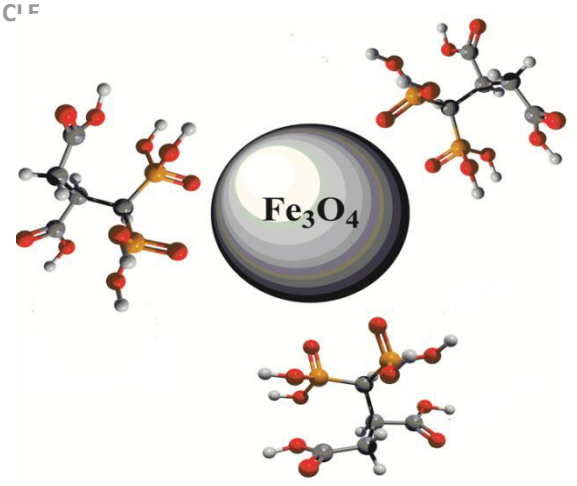

Figure 1 - Schematic depiction of Fe_3O_4-DPD MNPs

In this study, the interaction of Fe_3O_4-DPD MNPs (Fig. 1) with external magnetic field (MF) gradient was analyzed to test their potential for the possible application in hyperthermia treatment. The heating efficiency of MNPs in biological conditions remains poorly understood, especially regarding the influence of their dispersion state. Hence, the behavior of Fe_3O_4-DPD MNPs in non-alternating external MF, by constant measuring of laser beam transparency through ferrofluid sample was monitored. These measurements were carried out before switching on MF, when the field was applied and after the switching off MF. Using the transparency analysis of ferrofluid in non-alternating external MF and changing the ionic strengths of the sample, the combined effects of MF and electrolyte were monitored. This allows better comprehension of the behavior of Fe_3O_4-DPD MNPs in external MF, in the absence and the presence of an electrolyte, and consequently the more comprehensive understanding of hyperthermia. Furthermore, we described the advances of DPD coatings for the radiolabeling of MNPs with ^{99m}Tc for their potential application as agent for SPECT diagnostics and hyperthermia therapy as well as with ^{90}Y for dual hyperthermia-radionuclide based therapy.

2 Experimental

2,3-Dicarboxypropane-1,1-diphosphonic acid (DPD) was synthesized in the Laboratory for Radioisotopes of the Vinča Institute of Nuclear Sciences,[16] while other materials and reagents for the preparation of Fe_3O_4-DPD MNPs were purchased from commercial sources without further purification.

Synthesis and detailed physicochemical properties of Fe_3O_4-DPD MNPs were previously described.[7] Briefly, after synthesis of Fe_3O_4 MNPs by coprecipitation method, DPD water solution (Fe_3O_4:DPD=1:1) was added and the coating reaction was carried out overnight at room temperature. The excess of unreacted DPD was removed by dialysis against deionized water for one day.

^{99m}Tc ($t_{1/2}$ =6 h, E_γ = 140 keV) was freshly eluted from a ^{99}Mo/^{99m}Tc generator (Vinča Institute of Nuclear Sciences, Belgrade, Serbia).

$^{90}YCl_3$ was purchased from Polatom, Poland, in a no-carrier-added form (29.64 GBq/cm^3, in 0.05 mol/dm^3 HCl, 18.5 TBq/mg Y, according to the product specification).

2.1 MNPs characterization

The mean particle diameters were determined in the suspension of 20 µl of Fe_3O_4-DPD MNPs in 3 ml saline solution with ionic strengths between 0.05-1.0 mol/dm^3 by using Zeta–sizer Nano ZS with a 633 nm He–Ne laser (Malvern Instruments Inc, UK). Results are expressed as the Z average, representing an average hydrodynamic particle diameter. The measurements were performed at room temperature.

2.2 Measurements in alternating and non-alternating MF

The magnetic hyperthermia efficiency of Fe_3O_4-DPD MNPs was tested by using Commercial AC applicator (model DM100 by nB nanoscale Biomagnetics). The heat generation of the dispersions Fe_3O_4-DPD MNPs under alternating magnetic field (30 mT) and the resonant frequencies between 252–577 kHz was measured directly on the samples dispersed in water. The heating efficiency of MNPs (2 mg/ml) is defined as specific power absorption (SPA) and is calculated according to the following formula: $SPA = (C_p \cdot m_w/m_m) \cdot (\Delta T/\Delta t)$, where Cp is the specific heat capacity of the medium ($C_p \sim C_{water}$ = 4.18 J g^{-1} K^{-1}), m_w and m_m are the masses of the medium (water) and magnetic nanoparticles, while $\Delta T/\Delta t$ is the initial slope of the time-dependent temperature curve.[17]

For the analysis in non-alternating external MF, device developed in our laboratory was used.[18] Sanyo laser diode DL5147-040 in the single mode regime at wavelength λ= 655nm was applied. Transmitted laser light was measured with a photodiode.

2.3 Radiolabeling of Fe_3O_4-DPD MNPs

2.3.1 ^{99m}Tc-labeling

Radiolabeling of Fe_3O_4-DPD MNPs was performed with ^{99m}Tc using $SnCl_2$ as a reducing agent. 100 µl of $Na^{99m}TcO_4$ (18.5 MBq) and 50 µl of freshly prepared tin(II)-solution (50 mg of $SnCl_2x2H_2O$ in 5 ml of 0.1 mol/dm^3 HCl) were added to the suspension of 50 µl of Fe_3O_4-DPD MNPs (5 mg/ml) in 1 ml of distilled water. The mixture was immediately adjusted with 0.1 mol/dm^3 HCl to pH 6 and gently stirred at room temperature for 30 min.

View Article Online
DOI: 10.1039/C8NJ06478D

Radiolabeled Fe_3O_4-DPD MNPs were then separated from free ^{99m}Tc by precipitation with the help of a permanent magnet. The radiolabeling yield of the ^{99m}Tc-Fe_3O_4-DPD MNPs was determined as the ratio of the measured radioactivity retained in the precipitate after magnetic separation and the known radioactivity used for the radiolabeling. The radioactivity was measured using a CRC-15 beta dose calibrator (Capintec Ramsey, NJ, USA) and gamma counter Wizard 2480 (Perkin Elmer, USA). Another method used for the measuring of radiolabeling yield was ascending instant thin-layer chromatography (ITLC) on silica gel (SG) coated fiber sheets. Using acetone as the mobile phase free $^{99m}TcO_4^-$ migrates to the front of the ITLC strip (Rf = 0.8–1.0) leaving the reduced/hydrolyzed ^{99m}Tc along with the radiolabeled complex (^{99m}Tc–MNPs) at the origin. In the mixture of pyridine:acetic acid:water (3:5:1.5), ^{99m}Tc-hydrolyzate remained at the origin, while both free $^{99m}TcO_4^-$ and ^{99m}Tc–Fe_3O_4-DPD MNPs migrated with the solvent front. The final percentage of the formed ^{99m}Tc–MNPs complex was determined based on the calculation of radiochemical purity in both systems.

2.3.2 ^{90}Y labeling

^{90}Y labeling of Fe_3O_4-DPD MNPs was performed using the method previously applied for the radiolabeling of phosphate coated MNPs.[19] Briefly, $^{90}YCl_3$ solution (6 µl, containing approximately 185 MBq) was added to an aqueous suspension of 5 mg/ml Fe_3O_4-DPD MNPs at pH 4-5 and incubated at room temperature on a shaker for 1 h.

Magnetic decantation and ITLC, performed on SG sheets with saline as the mobile phase, were used to quantify the radiolabelling yield. In this system, ^{90}Y-labeled MNPs remained at the origin (Rf = 0.0–0.1), while the unbound $^{90}Y^{3+}$ migrated with the solvent front (Rf = 0.8–0.9). Since ^{90}Y is a pure β-emitter it can only be detected by the measured ''bremsstrahlung''[20,21] in a dose calibrator or gamma counter. All measurements were carried out under the same geometric conditions.

2.4 *In vitro* stability testing

The *in vitro* stability of radiolabeled MNPs (50 µl) was tested in different solutions (1 ml): saline (0.9 % NaCl), human serum (4% water solution of human serum albumin) and 0.01 mol/dm^3 DTPA solution, after incubation at 37 ^{0}C over a period of 24 h for ^{99m}Tc-Fe_3O_4-DPD MNPs and over a period of 72 h for ^{90}Y-Fe_3O_4-DPD MNPs. Small amounts of sample were taken at different time points and analyzed by ITLC-SG using above mentioned mobile phases.

2.5 Biodistribution and *in vivo* stability studies

Biodistribution studies were carried out in healthy male 4-week old Wistar rats (100 ± 10 g body weight, Laboratory for Biology, Vinča Institute of Nuclear Sciences) according to the guidelines of the European Council Directive (86/609/EEC) and the Serbian Laboratory Animal Science Association (SLASA). Radiolabeled MNPs were intravenously injected through the tail vein in a maximum volume of 0.15 ml (0.3 mg Fe_3O_4-DPD MNPs in saline, approx. 2.5 MBq). The animals were sacrificed at the following time points (t = 0.5, 1, 2 and 24 h) for ^{99m}Tc-Fe_3O_4-DPD and (t = 0.5, 1, 24 and 72 h) for ^{90}Y-Fe_3O_4-DPD MNPs by cervical dislocation. The results of the uptake into organs were expressed as a percentage of the injected activity per gram (% ID/g) and per ml of blood, when compared with appropriate standards for the injected dose (ID).

The Ethical Committee of the Vinča Institute of Nuclear Sciences, University of Belgrade, approved this study, and permission was obtained according to the Law for Animal Welfare from the Ministry of Agriculture and Environmental Protection, Republic of Serbia (permission number 323-07-04725/2018-05).

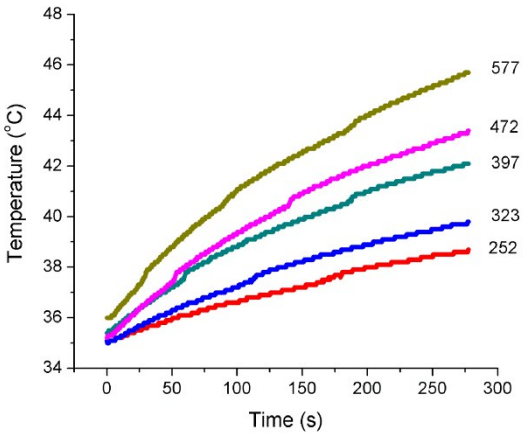

Figure 2 - Heating capacity of Fe_3O_4-DPD MNPs at 30mT and different field frequencies

3 Results and discussion

3.1 Measurements in alternating and non-alternating MF

For medical applications of magnetic hyperthermia, physiological limitations should be well-thought-out. High-frequency MF can cause local heating in the part of the tissue where no magnetic particles were found, owing to the eddy currents. Besides clinical limitations, technical limitations should be also kept in mind, as most of studies on biological specimens take place in a narrow range of frequencies. The applied frequencies, along with the amplitude of the AC field are generally grounded on literature data. In the absence of a better criterion, most of the authors cite papers by *Atkinson*[22] and *Brezovich*.[23]

The temperature increase of Fe_3O_4-DPD MNPs (2 mg/ml) as a function of the time was evaluated under different frequencies 252–577 kHz and a magnetic field strength of 30 mT (Fig.2). From the temperature curve, it was observed that Fe_3O_4-DPD MNPs shows heating effect even at 252 kHz.

Besides the applied frequency and field strength, physicochemical characteristics of the sample such as particle size and shape as well as the concentration of the sample strongly affect the behavior of MNPs both in alternating and

View Article Online
DOI: 10.1039/C8NJ06478D

Table1 - SPA values of Fe_3O_4-DPD MNPs at different concentrations (397 kHz, 30 mT)

Concentration (mg/ml)	SPA (W/g)
0.25	0
0.5	0
1	0
2	81
5	91
8	92

non-alternating MF. Generally, higher concentrations of MNPs widen the application of different electric and magnetic fields.[24] By dilution of the Fe_3O_4-DPD ferrofluid SPA values decrease and at concentrations below 2 mg/ml hyperthermia effect could not be observed (Table 1).

The behavior of Fe_3O_4-DPD MNPs in non-alternating MF (30 mT) for different concentrations is depicted in Fig. 3.The detail explanation of the effect has been described in previous paper[18], hence only the basic theoretical considerations have been given here. Regardless of the concentration used, at the beginning of the measuring, when the MF is switched-off, the sample has shown the initial transparency. At the point, when the MF is switched-on, a swift decrease of intensity of transmitted light was observed. The width and depth of the valley depend on the used MF and on the type of ferrofluid, as observed previously[18]. After some time rapid increase in the intensity of transmitted light occurs. At a certain point, the saturation effect has been noticed.

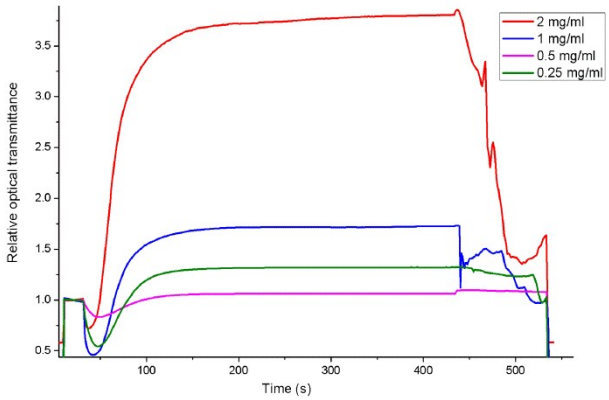

Figure 3 -Time dependence of transmitted diode laser light (λ=655 nm) for different concentrations of the sample at magnetic field strength of 30 mT.

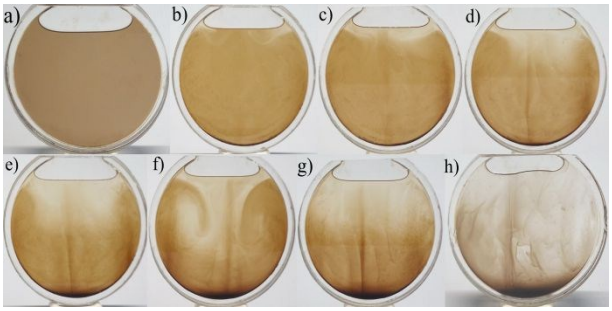

Figure 4 - Fe_3O_4-DPD MNPs sample: a) In the absence of non-alternating MF; b)-g) In the presence of non-alternating MF (30 mT); h) At the saturation point

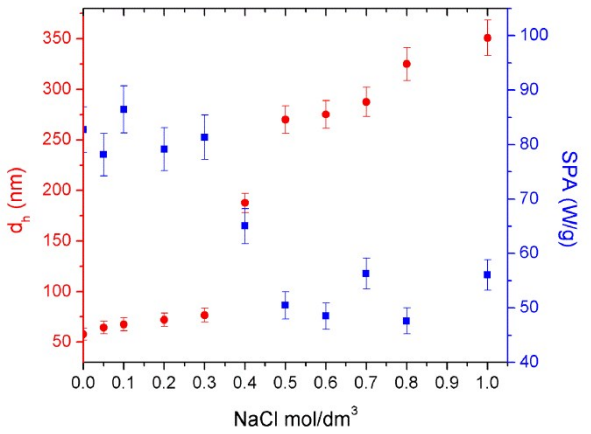

Figure 5 -The dependence of SPA values and hydrodynamic diameter on ionic strength at 30 mT and 397 kHz.

This rise of the intensity is according to the model[25] and is due to the orientation of the magnetic domains of nanoparticles caused by MF.

Non-alternating MF forces magnetic particles along the field lines, likewise magnetic needles. Magnetic domains ordered in such a manner are attracted forming magnetic chains. Further on, the chains can be organized to form a quasi-lattice of magnetic threads. This aggregation process depends on the field strength and the time interval of the exposure. During the time, the sizes of scatterers increase due to the formation of doublets, triplets or very small chains[25-31]. At a certain time point, a number of scatterers sizes satisfy the resonances in the scattering anisotropy and extinction efficiency factors. At the minimum transparency, the number of caterers satisfying the resonance becomes maximum. When MF was switched off, the sample becomes more transparent and the intensity of transmitted light increases rapidly. This is due to theadditional attachment of free magnetic nanoparticles in the solution and their embedding into magnetic chains.Precipitation of the sample during the time in the non-alternating MF has been depicted in Fig. 4.

Monitoring the effect of non-alternating MF by measuring the transparency of the Fe_3O_4-DPD ferrofluid, was not possible at concentrations ≥ 5 mg/ml due to the high density of the sample. At the highest tested concentration (2 mg/ml) the ratio between well depth and height of transparency increase is the largest (Fig.3). Also, the width of the well is the smallest for the highest concentrations. By dilution of the sample (1 mg/ml and 0.5 mg/ml) the ratio between well depth and height of transparency increase has been decreased. At the same time the width of the well increases. At the lowest concentrations (0.25 mg/ml), the increase of transparency is very small reaching only the initial value (when the MF was switched-off). Below 2 mg/ml the heating capacity of the sample has not been observed and also the drastic change of curve profiles in non-alternating MF has been noticed.

The addition of sodium chloride to the ferrofluid sample drastically affects their behavior in both alternating and non-alternating MF. Strong aggregation of coated nanoparticles,

characterized by a steep increase in hydrodynamic diameter, occurs when the ionic strength reaches a value of 0.4 mol/dm^3(Fig.5). The process of aggregation is getting stronger with the further increase of NaCl concentration. Bellow the 0.4 mol/dm^3 the change of hydrodynamic diameter is less intense. The aggregation process is associated with simultaneous changes in SPA values. At 0.4 mol/dm^3 drastic decline have been observed. In the concentration range of 0.5-1.0 mol/dm^3 NaCl, the decrease of 45 %, with respect to SPA values measured for ionic strength 0-0.3 mol/dm^3 occurred.

At higher ionic strengths (higher NaCl concentrations), the Fe_3O_4-DPD MNPs became less stable compared to the lower ionic strengths. This indicates that the thickness of the DPD coating on the Fe_3O_4 surface is not high enough to stabilize the particles. In Fig.5, it has been shown that the hydrodynamic diameter increases at high salt concentration, which results in agglomeration and precipitation. At a low salt concentration, the repulsive forces are dominant over the attractive forces and the particle size was not changed significantly. By the increase of the ionic strength, the decrease in the electron-alternating forces occur, rising the receptiveness of the dispersed particles to form aggregates.[11,32]

In non-alternating MF, regardless of NaCl concentration, initial transparency of the sample (when a magnetic field is switched-off) decreases with time (Fig.6). The increase of NaCl concentration up to 0.5 mol/dm^3 leads to the blurring of ferrofluid, i.e. the initial transparency is higher for lower concentrations of NaCl. At concentrations higher than 0.5 mol/dm^3 the adverse effect was observed since the precipitation of magnetic particles is larger as showed with DLS measurements (Fig.5).

At the time when MF was switched-on the abrupt depression of transparency of all samples was observed. The effect of MF on magnetic particles in solution, i.e. the increase of transparency is the largest for the ferrofluid sample without NaCl. Addition of small amounts of NaCl (0.05-0.3 mol/dm^3) drastically changes transparency values. It is obvious that even small concentrations of electrolyte interfere with the magnetic field effect. However, up to 0.3 mol/dm^3, all curves have a similar convex shape. For concentrations higher than 0.3 mol/dm^3 the shape of the curves is different. At a concentration of 0.4 mol/dm^3, the increase of transparency showed the nearly linear path. For the concentration range of 0.6-1.0 mol/dm^3, the curves are concave. The observed effect of MF on magnetic particles is drastically weaker in the concentration range of 0.4-1.0 Mol/dm^3, compared to lower concentrations of NaCl. The higher concentrations of NaCl lead to increased precipitation of magnetic particles, which makes them difficult to orientate with respect to MF and to create magnetic chains under field effect, as explained previously.[18,25–31]

The larger aggregation of MNPs due to the presence of electrolyte leads to the increase of magnetic interactions between nanoparticles and magnetic response with respect to the external field is diminished. As a consequence, change in the transparency profile of the sample and decrease of hyperthermia efficiency was observed. Furthermore, the demagnetizing field induced within the aggregates due to their magnetization, decreases the local magnetic field, leading to a reduction of transparency and SPA.[11]

In the range of the lower ionic strengths (0.05-0.3 mol/dm^3 NaCl) which are approximate to the physiological conditions, negligible changes in hydrodynamic diameters and SPA values of MNPs have been observed. In accordance, the measurements in the non-alternating MF for the same concentration range have shown the curve profiles which do not differ from one another significantly up to a concentration of 0.4 mol/dm^3 NaCl.

3.2 Radiolabeling of Fe_3O_4-DPD MNPs

The radiotracer technique is a relevant approach for studying uptake, distribution and biodegradation of newly designed nanoparticles. BPs bind very strongly to the surface of magnetic nanoparticles allowing further labeling with diagnostic and therapeutic radionuclides.[19,33] In our previous work[7], design, synthesis, characterization and radiolabeling of a Fe_3O_4-DPD MNPs with the positron emitter ^{68}Ga were described showing their high potential as an imaging agent for PET/MRI.

Radiolabeling of Fe_3O_4-DPD MNPs was possible with both examined radionuclides ^{99m}Tc and ^{90}Y, using the chelator-free radiolabeling method. These radionuclides make stable complexes with a variety of groups that are present on the nanoparticle surface.[34] Radiolabeling of Fe_3O_4-DPD MNPs was performed at high yields (>98 % for ^{99m}Tc and >93 % for ^{90}Y), as in the case of other BPs coated nanoparticles.[19,33] This was expected,considering that DPD, as a tetradentate ligand with two phosphonates and two carboxylates, is a suitable ligand for direct labeling with radiometals.[15]

Table 2: *In vitro* stability of ^{99m}Tc-Fe_3O_4-DPD MNPs during 24 h at 37 °C in different incubation medium: saline, human serum and 0.01 mol/dm^3 DTPA.

Incubation medium	Radiochemical purity, RCP (%)				
	Incubation time				
	0.5 h	1 h	2 h	6 h	24 h
Saline	98.6	98.1	98.0	96.1	92.9
Human serum	93.7	92.4	91.3	88.9	84.2
DTPA	98.5	98.0	97.7	95.8	91.5

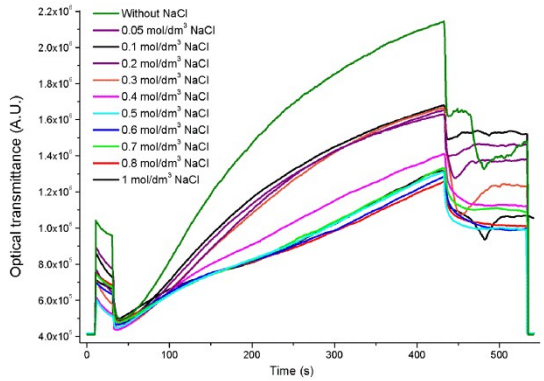

Figure 6 -Time dependence of transmitted diode laser light (λ=655 nm) for different ionic strengths at magnetic field strength of 30 mT

View Article Online
DOI: 10.1039/C8NJ06478D

Table 3: *In vitro* stability of ^{90}Y-Fe_3O_4-DPD MNPs during 72 h at 37 °C in different incubation medium: saline, human serum and 0.01 mol/dm^3 DTPA.

Incubation medium	Radiochemical purity, RCP (%)				
	Incubation time				
	0.5 h	1 h	24 h	48 h	72 h
Saline	93.1	92.8	91.5	89.3	87.6
Human serum	91.4	90.7	87.6	84.1	79.4
DTPA	93.3	93.1	92.5	91.5	91.3

3.3 *In vitro* stability of radiolabeled Fe_3O_4-DPD MNPs

With the aim of assessing the *in vitro* stability of radiolabeled Fe_3O_4-DPD MNPs in biological media, they were incubated in saline, human serum and DTPA solution at 37 °C during a certain period of time. The proportion of the total radioactivity in the sample presented in the form of the desired radioactive nanoprobe (^{99m}Tc-Fe_3O_4-DPD MNPs) is expressed as radiochemical purity, RCP (Tables 2 and 3). The RCP values of ^{99m}Tc- Fe_3O_4-DPD MNPs determined after 24 h incubation in saline, human serum and DTPA solution (92.9 %, 84.2 % and 91.5 %, respectively), showed that ^{99m}Tc-Fe_3O_4-DPD MNPs exhibited excellent *in vitro* stability, regardless the incubation conditions.

A negligible amount of ^{90}Y was lost from the radiolabeled MNPs after 72 h incubation in all tested media, showing RCP 87.6 %, 79.4 % and 91.3 % for saline, human serum and DTPA, respectively. This indicated that ^{90}Y-Fe_3O_4-DPD MNPs remained stable for at least 3 days under physiological conditions.

Similar results were obtained for ^{68}Ga-Fe_3O_4-DPD MNPs after 2 h incubation in PBS and human serum, showing RCP values > 80 %.[7]

3.4 Biodistribution Studies

Biodistribution and clearance of nanoparticles depend on their chemical and biochemical properties such as size, surface functionality and charge.[35,36] In general, it is well-established that nanoparticles are taken up by the RES system following i.v. administration, leading to the clearance of nanoparticles from systemic circulation.[37] Biodistribution of Fe_3O_4-DPD MNPs was studying over 24 h and 72 h after i.v. injection of ^{99m}Tc-Fe_3O_4-DPD and ^{90}Y-Fe_3O_4-DPD MNPs respectively, by measuring the radioactivity of the radiolabeled compounds in various tissues.[37-39] It was possible to compare the biodistribution profiles obtained by using two radioisotopes in order to confirm the efficiency and *in vivo* stability of the radiolabeled MNPs. ^{90}Y with a half-life of 2.8 days was used for the biodistribution analysis over 3 days, while ^{99m}Tc is not suitable for long time biodistribution evaluation due to 6 h half-life. Tissue distribution expressed as the percentage of injected dose per gram tissue is presented in Fig.7. High accumulation of MNPs was mainly observed in the liver 1 h after i.v. administration (16.03 % ID/g for ^{99m}Tc-Fe_3O_4-DPD and 11.28 % ID/g for ^{90}Y-Fe_3O_4-DPD MNPs) as well as the long-term retention in the same organ. Low accumulation of both radiolabeled nanoprobes in lungs was observed. These results demonstrate that hydrophilic DPD coating prevents Fe_3O_4 MNPs aggregation under *in vivo* conditions, as is the case with naked MNPs.[40] Owing to the fact that trivalent radiometals such as yttrium are predominantly taken from circulation by bones,[41] low release of ^{90}Y from radiolabeled MNPs was proved by insignificant bone uptake indicating *in vivo* stability of ^{90}Y-Fe_3O_4-DPD MNPs. Also, due to the *in vivo* stability of ^{99m}Tc-Fe_3O_4-DPD MNPs, the insignificant radioactivity in the stomach at all time-points was observed.

Conclusions

The interaction of Fe_3O_4-DPD MNPs with alternating external magnetic field is of special interest due to their possible application in hyperthermia treatment. The results presented imply that the DPD-coated MNPs could maintain their heating capacity in the range of 252-577 kHz and thus have potential in biomedical applications.

Further, for the better understanding of hyperthermia, the interaction of Fe_3O_4-DPD MNPs with a non-alternating magnetic field was examined. An increase of ionic strength of samples leads to the aggregation of MNPs. This process has been monitored by measuring of SPA values, hydrodynamic

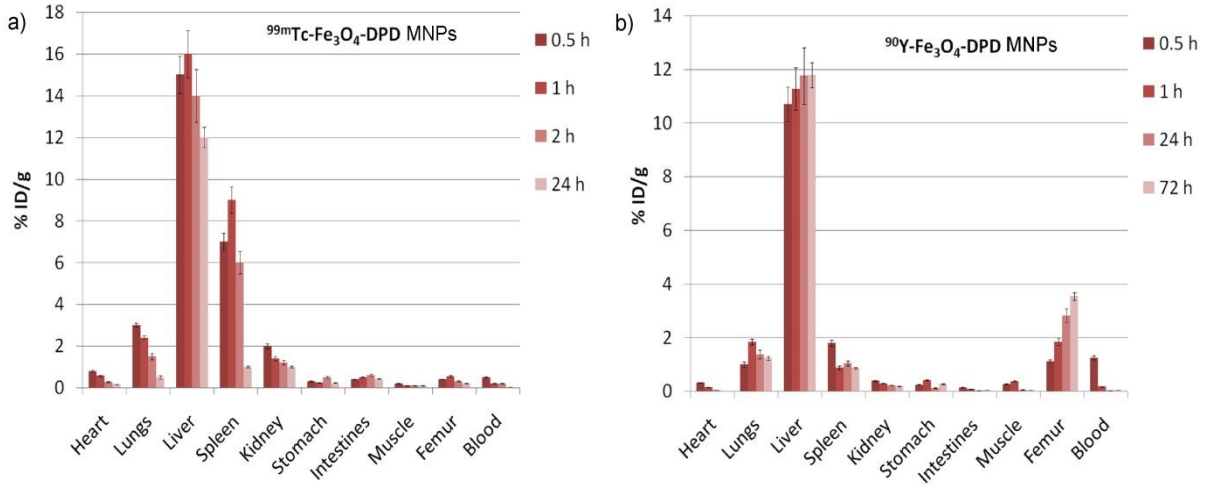

Figure 7 -Biodistribution of a) ^{99m}Tc-Fe_3O_4-DPD and b) ^{90}Y-Fe_3O_4-DPD MNPs after intravenous administration in normal Wistar rats (% ID/g)

diameter and transparency in the non-alternating field. Within the range of 0.05-0.3 mol/dm^3 NaCl, similar to the physiological conditions, minor changes in hydrodynamic diameters and SPA values have been observed. In an agreement, the measurements in the non-alternating MF for the same concentration range have shown a similar trend up to a concentration of 0.4 mol/dm^3 NaCl. Transparency measurement of Fe_3O_4-DPD MNPs in non-alternating MF clarified the mechanism of particle aggregation before switching on MF, when the field is applied and after the switching off MF. These measurements gave us insight into the orientation of magnetic domains and aggregate formation in the absence and the presence of electrolyte which allows a more comprehensive understanding of hyperthermia.

Coated MNPs were radiolabeled for two purposes: to use the radiotracer to obtain an accurate biodistribution profile of the Fe_3O_4-DPD MNPs and to investigate the preparation of the potential therapeutic and diagnostic agents. ^{90}Y-Fe_3O_4-DPD and ^{99m}Tc-Fe_3O_4-DPD MNPs were obtained in high radiolabeling yield and exhibited high *in vitro* stability in saline, human serum and DTPA solution. The results of biodistribution showed high uptake in the liver and spleen after i.v. administration as well as *in vivo* stability and long retention in these organs. Radiolabeled Fe_3O_4-DPD MNPs with different metallic radionuclides such as ^{99m}Tc and ^{90}Y, seem to hold great potential as theranostic agents with improved diagnostic and therapy abilities.

Conflicts of interest

There are no conflicts to declare.

Acknowledgments

The Ministry of Education, Science and Technological Development of the Republic of Serbia supported this work financially through the Project Grant No. III 45015, 172035, 171034 and FP7-ERAChairs-PilotCall-2013, MAGBIOVIN.

References

1 C. C. Berry and A. S. G. Curtis, Functionalisation of magnetic nanoparticles for applications in biomedicine, *J. Phys. D Appl. Phys*, 2003, **36**, 198–206.

2 S. Dutz, R. Hergt, J. Mürbe, R. Müller, M. Zeisberger, W. Andrä, J. Töpfer and M. E. Bellemann, Hysteresis losses of magnetic nanoparticle powders in the single domain size range, *J. Magn. Magn. Mater.*, 2007, **308**, 305–312.

3 H. Mamiya and B. Jeyadevan, Hyperthermic effects of dissipative structures of magnetic nanoparticles in large alternating magnetic fields, *Sci. Rep.*, 2011, **1 (157)**, 1-7.

4 B. B. Lahiri, T. Muthukumaran and J. Philip, Magnetic hyperthermia in phosphate coated iron oxide nanofluids, *J. Magn. Magn. Mater.*, 2016, **407**, 101–113.

5 H. Zolata, H. Afarideh and F. A. Davani, Triple Therapy of HER2 $^+$ Cancer Using Radiolabeled Multifunctional Iron Oxide Nanoparticles and Alternating Magnetic Field, *Cancer Biother. Radiopharm.*, 2016, **31**, 324–329.

6 S. Same, A. Aghanejad, S. Akbari Nakhjavani, J. Barar and Y. Omidi, Radiolabeled theranostics: magnetic and gold nanoparticles., *Bioimpacts*, 2016, **6**, 169–181.

7 M.-A. Karageorgou, S. Vranješ-Djurić, M. Radović, A. Lyberopoulou, B. Antić, M. Rouchota, M. Gazouli, G. Loudos, S. Xanthopoulos, Z. Sideratou, D. Stamopoulos and P. Bouziotis, Gallium-68 Labeled Iron Oxide Nanoparticles Coated with 2,3-Dicarboxypropane-1,1-diphosphonic Acid as a Potential PET/MR Imaging Agent: A Proof-of-Concept Study., *Contrast Media Mol. Imaging*, 2017, **2017**, 6951240–6951253.

8 D.-E. Lee, H. Koo, I.-C. Sun, J. H. Ryu, K. Kim and I. C. Kwon, Multifunctional nanoparticles for multimodal imaging and theragnosis., *Chem. Soc. Rev.*, 2012, **41**, 2656–72.

9 J. Fatisson, I. R. Quevedo, K. J. Wilkinson and N. Tufenkji, Physicochemical characterization of engineered nanoparticles under physiological conditions: Effect of culture media components and particle surface coating, *Colloids Surfaces B Biointerfaces*, 2012, **91**, 198–204.

10 M. Safi, J. Courtois, M. Seigneuret, H. Conjeaud and J.-F. Berret, The effects of aggregation and protein corona on the cellular internalization of iron oxide nanoparticles, *Biomaterials*, 2011, **32**, 9353–9363.

11 D. S. Nikam, S. V. Jadhav, V. M. Khot, R. S. Ningthoujam, C. K. Hong, S. S. Mali and S. H. Pawar, Colloidal stability of polyethylene glycol functionalized Co0.5Zn0.5Fe2O4 nanoparticles: effect of pH, sample and salt concentration for hyperthermia application, *RSC Adv.*, 2014, **4**, 12662–12671.

12 T. Muthukumaran and J. Philip, Effect of phosphate and oleic acid capping on structure, magnetic properties and thermal stability of iron oxide nanoparticles, *J. Alloys Compd.*, 2016, **689**, 959–968.

13 T. Muthukumaran and J. Philip, A Single Pot Approach for Synthesis of Phosphate Coated Iron Oxide Nanoparticles, *J. Nanosci. Nanotechnol.*, 2015, **15**, 2715–2725.

14 M. Vorne, S. Vähätalo and T. Lantto, A clinical comparison of 99mTc-DPD and two 99mTc-MDP agents, *Eur. J. Nucl. Med.*, 1983, **8**, 395–397.

15 D. D. Djokić, D. L. Janković and N. S. Nikolić, Labeling, characterization, and in vivo localization of a new 90Y-based phosphonate chelate 2,3-dicarboxypropane-1,1-diphosphonic acid for the treatment of bone metastases: Comparison with 99mTc–DPD complex, *Bioorg. Med. Chem.*, 2008, **16**, 4457–4465.

16 N. Vanlic-Razumenic and N. Vukicevic, The synthesis and physico-chemical properties of 2,3-dicarboxypropane-1,1-diphosphonic acid, a ligand for preparing the 99mTc-labeled skeletal imaging agent, *J. Serbian Chem. Soc.*, 1986, 5163–5166.

17 P. B. Shete, R. M. Patil, N. D. Thorat, A. Prasad, R. S. Ningthoujam, S. J. Ghosh and S. H. Pawar, Magnetic chitosan nanocomposite for hyperthermia therapy application: Preparation, characterization and in vitro experiments, *Appl. Surf. Sci.*, 2014, **288**, 149–157.

18 M. M. Kuraica, P. Iskrenović, M. Perić, I. Krstić and A. S. Nikolić, External magnetic field influence on magnetite and cobalt-ferrite nano-particles in ferrofluid, *Chem. Pap.*, 2018, **72**, 1535–1542.

19 M. Radović, M. Mirković, M. Perić, D. Janković, A. Vukadinović, D. Stanković, Đ. Petrović, M. Bošković, B. Antić, M. Marković and S. Vranješ-Đurić, Design and preparation of ^{90} Y-labeled imidodiphosphate- and inositol hexaphosphate-coated magnetic nanoparticles for possible medical applications, *J. Mater. Chem. B*, 2017, **5**, 8738–8747.

20 H. C. Manjunatha and B. Rudraswamy, Exposure of bremsstrahlung from beta-emitting therapeutic radionuclides, *Radiat. Meas.*, 2009, **44**, 206–210.

21 H. C. Manjunatha and B. Rudraswamy, Bremsstrahlung exposure of tissues from beta-therapeutic nuclides, *Nucl. Instruments Methods Phys. Res. Sect. A Accel. Spectrometers, Detect. Assoc. Equip.*, 2010, **621**, 581–589.

22 W. J. Atkinson, I. A. Brezovich and D. P. Chakraborty, Usable Frequencies in Hyperthermia with Thermal Seeds, *IEEE Trans. Biomed. Eng.*, 1984, **31**, 70–75.

23 I. Brezovich, Low frequency hyperthermia: capacitive and ferromagnetic thermoseed methods, *Med. Phys. Monogr.*, 1988, **16**, 82–111.

24 S. Spirou, S. Costa Lima, P. Bouziotis, S. Vranješ-Djurić, E. Efthimiadou, A. Laurenzana, A. Barbosa, I. Garcia-Alonso, C. Jones and D. Jankovic, Recommendations for In Vitro and In Vivo Testing of Magnetic Nanoparticle Hyperthermia Combined with Radiation Therapy, *Nanomaterials*, 2018, **8**, 306.

25 J. Li, X.-D. Liu, Y.-Q. Lin, Y. Huang and L. Bai, Relaxation behavior measuring of transmitted light through ferrofluids film, *Appl. Phys. B*, 2006, **82**, 81–84.

26 X. Bai, S. Pu and L. Wang, Optical relaxation properties of magnetic fluids under externally magnetic fields, *Opt. Commun.*, 2011, **284**, 4929–4935.

27 S. Brojabasi, T. Muthukumaran, J. M. Laskar and J. Philip, The effect of suspended Fe3O4 nanoparticle size on magneto-optical properties of ferrofluids, *Opt. Commun.*, 2015, **336**, 278–285.

28 J. M. Laskar, J. Philip and B. Raj, Experimental evidence for reversible zippering of chains in magnetic nanofluids under external magnetic fields, *Phys. Rev. E*, 2009, **80**, 41401.

29 S.-D. Li and L. Huang, Nanoparticles evading the reticuloendothelial system: role of the supported bilayer., *Biochim. Biophys. Acta*, 2009, **1788**, 2259–66.

30 J. Philip and J. M. Laskar, Optical Properties and Applications of Ferrofluids—A Review, *J. Nanofluids*, 2012, **1**, 3–20.

31 Y. Huang, D. Li, F. Li, Q. Zhu and Y. Xie, Transmitted light relaxation and microstructure evolution of ferrofluids under gradient magnetic fields, *Opt. Commun.*, 2015, **338**, 551–559.

32 C. Guibert, V. Dupuis, V. Peyre and J. Fresnais, Hyperthermia of Magnetic Nanoparticles: Experimental Study of the Role of Aggregation, *J. Phys. Chem. C*, 2015, **119**, 28148–28154.

33 R. Torres, R. Tavaré, A. Glaria, G. Varma, A. Protti, P. Blower, ^{99m}Tc-Bisphosphonate-Iron Oxide Nanoparticle Conjugates for Dual-Modality Biomedical Imaging, *Bioconjugate Chem.*, 2011, **22**, 455-465.

34 D. Psimadas, P. Bouziotis, P. Georgoulias, V. Valotassiou, T. Tsotakos and G. Loudos, Radiolabeling approaches of nanoparticles with ^{99m}Tc, *Contrast Media Mol. Imaging*, 2013, **8**, 333–339.

35 S. Shanehsazzadeh, M. A. Oghabian, F. J. Daha, M. Amanlou and B. J. Allen, Biodistribution of ultra small superparamagnetic iron oxide nanoparticles in BALB mice, *J Radioanal Nucl Chem*, 2013, **295**, 1517–1523.

36 C. Gonçalves, M. F. M. Ferreira, A. C. Santos, M. I. M. Prata, C. F. G. C. Geraldes, J. A. Martins and F. M. Gama, Studies on the biodistribution of dextrin nanoparticles, *Nanotechnology*, 2010, **21**, 295103–295112.

37 N. Arulsudar, N. Subramanian, P. Mishra, R. K. Sharma and R. S. R. Murthy, Preparation, Characterisation and Biodistribution of 99m Tc-labeled Liposome Encapsulated Cyclosporine, *J. Drug Target.*, 2003, **11**, 187–196.

38 A. Babbar, R. Kashyap and U. P. Chauhan, A convenient method for the preparation of 99mTc-labelled pentavalent DMSA and its evaluation as a tumour imaging agent., *J. Nucl. Biol. Med.*, 1991, **35**, 100–4.

39 A. Bhatnagar, A. K. Singh, A. Babbar, N. L. Soni and T. Singh, Renal imaging with 99Tc(m)-dextran., *Nucl. Med. Commun.*, 1997, **18**, 562–6.

40 M. Radović, M. P. Calatayud, G. F. Goya, M. R. Ibarra, B. Antić, V. Spasojević, N. Nikolić, D. Janković, M. Mirković and S. Vranješ-Đurić, Preparation and *in vivo* evaluation of multifunctional ^{90}Y-labeled magnetic nanoparticles designed for cancer therapy, *J. Biomed. Mater. Res. Part A*, 2015, **103**, 126–134.

41 T. J. Wadas, E. H. Wong, G. R. Weisman and C. J. Anderson, Coordinating Radiometals of Copper, Gallium, Indium, Yttrium, and Zirconium for PET and SPECT Imaging of Disease, *Chem. Rev.*, 2010, **110**, 2858–2902.

View Article Online DOI: 10.1039/C9NJ00647BD

View Article Online
DOI: 10.1039/C8NJ06478D

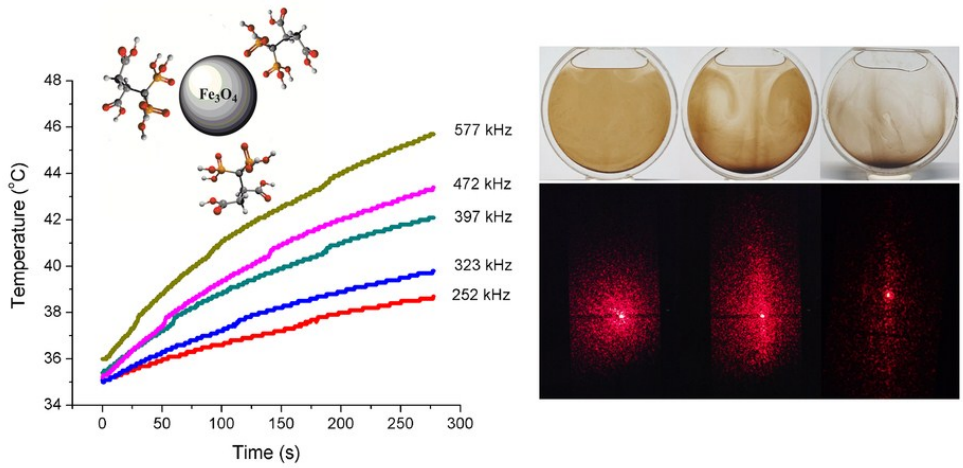

Measuring of laser transparency through the sampleof Fe_3O_4-DPD MNPsin non-alternating magnetic field, for comprehensive understanding of hyperthermia.

80x39mm (300 x 300 DPI)